REGULATORY INFORMATION DISTRIBUTION SYSTEM (RIDS)

ACCESSION NBR:8410040261 DOC.DATE: 84/09/28 NOTARIZED: NO DOCKET #
FACIL:50-250 Turkey Point Plant, Unit 3, Florida Power and Light C 05000250
50-251 Turkey Point Plant, Unit 4, Florida Power and Light C 05000251
AUTH.NAME AUTHOR AFFILIATION
WILLIAMS,J.W. Florida Power & Light Co.
RECIP.NAME RECIPIENT AFFILIATION
VARGA,S.A. Operating Reactors Branch 1

SUBJECT: Forwards response to 840813 request for addl info re proposed amend to spent fuel facility expansion.

DISTRIBUTION CODE: A001D COPIES RECEIVED:LTR 1 ENCL 1 SIZE: 27
TITLE: OR Submittal: General Distribution

NOTES: 05000250
OL:07/19/72
05000251
OL:04/14/73

	RECIPIENT ID CODE/NAME	COPIES LTTR	COPIES ENCL	RECIPIENT ID CODE/NAME	COPIES LTTR	COPIES ENCL
	NRR ORB1 BC 01	7	7			
INTERNAL:	ADM/LFMB	1	0	ELD/HDS4	1	0
	NRR/DE/MTEB	1	1	NRR/DL DIR	1	1
	NRR/DL/ORAB	1	0	~~NRR/DSI/METB~~	1	1
	NRR/DSI/RAB	1	1	REG FILE 04	1	1
	RGN2	1	1			
EXTERNAL:	ACRS 09	6	6	LPDR 03	1	1
	NRC PDR 02	1	1	NSIC 05	1	1
	NTIS	1	1			

TOTAL NUMBER OF COPIES REQUIRED: LTTR 26 ENCL 23

[illegible]

[illegible] fifty expressions.

[illegible]

P.O. BOX 14000, JUNO BEACH, FL 33408

FLORIDA POWER & LIGHT COMPANY

September 28, 1984
L-84-263

Office of Nuclear Reactor Regulation
Attention: Mr. Steven A. Varga, Chief
Operating Reactor Branch #1
Division of Licensing
U.S. Nuclear Regulatory Commission
Washington, D.C. 20555

Dear Mr. Varga:

Re: Turkey Points Units 3 & 4
Docket Nos. 50-250 & 50-251
Proposed Amendment to
Spent Fuel Storage Facility Expansion
Additional Information

By letter dated August 13, 1984, the NRC requested additional information regarding the structural design of the spent fuel pit and new storage racks. The attachment to this letter provides our responses to these NRC questions.

If you have any questions, please contact us.

Very truly yours,

J.W. Williams, Jr.
Group Vice President
Nuclear Energy

JWW/GJK/mp

Attachment

cc: J.P. O'Reilly, Region II
Harold F. Reis, Esquire

A001
1/1

FLORIDA POWER & LIGHT COMPANY
TURKEY POINT UNITS 3 & 4
PROPOSED AMENDMENT TO
SPENT FUEL STORAGE FACILITY EXPANSION
REQUEST FOR ADDITIONAL INFORMATION

1. Please provide the detailed seismic analysis report and relevant design drawing related to welds and support structure for review.

   RESPONSE: The detailed stress reports and relevant design drawings for the fuel racks constitute proprietary information and are maintained by the rack vendor (Westinghouse). All materials are available for your review and we welcome the opportunity to discuss with you any concerns or questions you may have.

2. Please identify the racks in Region I and II being analyzed.

   RESPONSE: The seismic analysis was performed for the 10x11 rack in Region I. This rack has a seven cell pad span in the N-S direction and a ten cell pad span in the E-W direction. The non-linear model was run using the seven cell pad span and did not result in the pads lifting off the floor. The other two Region I racks are 8x11 racks one of which has seven cell pad span N-S and ten cell pad span E-W and the other has six cell pad span N-S and ten cell pad span E-W. The 8x11 rack with the six cell pad span was investigated and was also found not to lift off the floor. Since all the racks have the same number of pads (four) the 10x11 rack will have the highest pad loads and rack stresses.

   A similar situtation occurs in Region II. The seismic analysis was performed for the 10x14 rack which has an 8x13 pad span. The non-linear analysis was run using the 8 cell pad span. The other racks in Region II with the pad spans are as follows: 3 racks 10x13 (3x12 pad span), 1 rack 9x14 (8x13 pad span), 3 racks 9x13 (8x12 pad span), and 1 rack 9x13 (7x12 pad span). The 9x13 rack with 7x12 pad spacing was investigated and found not to lift off the floor. Thus the 10x14 rack will have the highest pad loads and rack stresses.

3. a. Please identify the computer codes used to generate the simplified 2-D nonlinear model and the detailed 3-D linear model.

   RESPONSE: The WECAN computer code was used to generate the simplified 2-D nonlinear model and the 3-D detailed linear model.

   b. Please provide documents on these codes for review.

   RESPONSE: The general WECAN code has been reviewed by the NRC through the submittal of Westinghouse document WCAP-8929, "Benchmark Problem Solutions Employed for Verification of the WECAN Computer Program". For review of additional capabilities which pertain to the fuel rack nonlinear dynamic analysis, the following documents are available:

3. b. CONTINUED:

1. Shah, V.N. Gilmore, C.B., "Dynamic Analysis of a Structure with Coulomb Friction", ASME Paper Number 82-PVP-18, presented at the 1982 ASME Pressure Vessel Piping Conference, Orlando, FL, June 1982.

2. Gilmore, C.B., "Seismic Analysis of Freestanding Fuel Racks", ASME Paper Number 82-PVP-17, presented at the 1982 ASME Pressure Vessel Piping Conference, Orlando, FL, June 1982.

4. a. Please provide detailed stress and displacement results obtained in the analysis.

RESPONSE: The following constitute the results, rack displacements, sliding, and rocking stability obtained from the seismic analysis for both Region I and Region II. The support pad vertical displacements are used to calculate the overall rack module rocking for partial and full fuel loading conditions. However, lift off does not occur for the racks evaluated (Region I and Region II) yielding a factor of safety against overturn much greater than 1.5.

4. a. Continued:

RACK DISPLACEMENTS

SSE Seismic + Maximum Normal Thermal			REGION I	REGION II
	SSE Seismic + Normal Thermal			
Max. Sliding Distance, μ = .2 (N-Linear Results)	Δs	in	.0001	0.007
Max. Structural Defl., μ = .8 (N-Linear Results)	δ	in	.124	0.086
Total Displacement One Rack $\Delta = \Delta s + \delta$	Δ	in	.1241	0.093
SSRS Combined Displacement 2 Racks with only 1 sliding $\Delta max = \sqrt{\Delta^2 + \delta^2}$	Δ max	in	.175	0.127
Max. Normal Thermal Displacement	δ_T	in	.088	0.087
Max. Combined Thermal & Seismic Displacements $\bar{\Delta} = \delta_T + \Delta max$	$\bar{\Delta}$	in	.256	0.214
Rack to Rack Gap	GAP	in	1.11	1.11

SSE Seismic Sliding + Max Accident Thermal			REGION I	REGION II
	SSE Seismic Sliding + Thermal Accident			
Max. Sliding Distance, μ = .2	Δs	in	.0001	0.007
Max. Accident Thermal Displacement	δ_T	in	.175	0.190
Combined Thermal & Seismic Sliding $\bar{\Delta} = \Delta_s + \delta_T$	$\bar{\Delta}$	in	.1751	0.197
Rack to Rack Gap	GAP	in	1.11	1.11

NOTE: THE RACK TO WALL GAPS ARE LARGER THAN THE RACK TO RACK GAPS.

4. a. <u>CONTINUED:</u>

COMPARISON OF LINEAR AND NON LINEAR MODEL PAD LOADS

REGION I 10x11

NS + DW

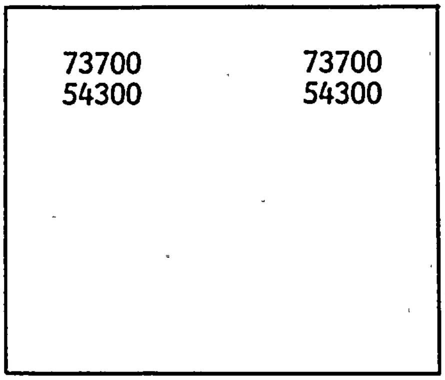

	Linear	Non Linear
Total NS + DW	147400	149600
Total DW	108600	112800
Ratio (NS+DW)/ DW	1.36	1.33

EW + DW

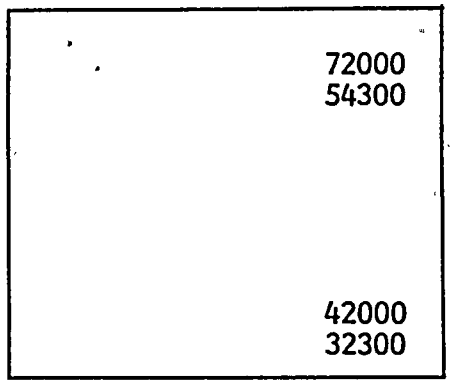

	Linear	Non Linear
Total EW + DW	114000	117000
Total DW	86600	88000
Ratio (EW+DW)/ DW	1.32	1.33

REGION II 10x14

NS + DW

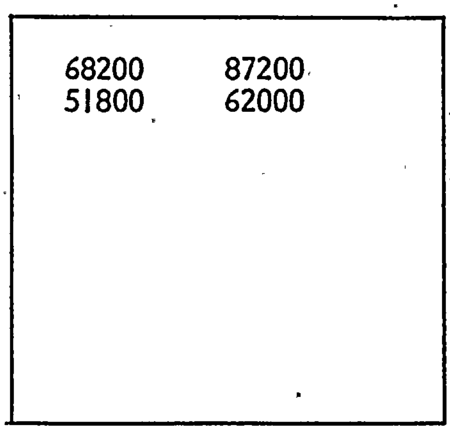

	Linear	Non Linear
Total NS + DW	155400	145300
Total DW	113800	101900
Ratio (NS+DW)/DW	1.37	1.43

EW + DW

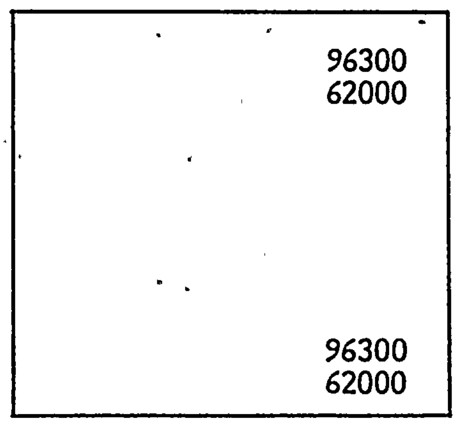

	Linear	Non Linear
Total ED + DW	192600	181600
Total DW	124000	114500
Ratio (EW+DW)/DW	1.55	1.59

4. b. Also provide the margins of safety for the maximum stresses under various seismic loading conditions.

RESPONSE:

REGION I RACKS

SUMMARY OF DESIGN STRESSES AND MINIMUM MARGINS OF SAFETY

Normal & Upset Conditions

	Design Stress (psi)	Allowable Stress (psi)	Margin of Safety
1.0 Support Pad Assembly			
1.1 Support Pad			
Shear	2009	23150*	10.52
Axial and Bending	5701	23150*	3.06
Bearing	4230	23150*	4.47
1.2 Support Pad Screw			
Shear	3675	9260	1.52
1.3 Support Plate			
Shear	2152	9260	3.30
Weld Shear	15672	23150*	.48
2.0 Cell Assembly			
2.1 Cell to Bottom Grid Weld			
Weld Shear	15840	23150*	.46
2.2 Cell to Top Grid Weld			
Weld Shear	15840	23150*	.46
2.3 Cell			
Axial and Bending	.514	1.0**	.94
2.4 Cell to Wrapper Weld			
Weld Shear	4517	9260	1.05
3.0 Grid Assembly			
3.1 Top Grid Box Member			
Shear	2055	9260	3.51
Axial and Bending	1659	13890	7.37
3.2 Top Grid Members			
Weld Shear	13544	21000	.55
3.3 Top Grid Outer Member			
Axial and Bending	1707	13890	7.14
Shear	146	9260	62.51
3.4 Bottom Grid Structure			
Shear	3349	9260	1.77
Axial and Bending	12057	13890	.15
3.5 Bottom Grid Members Welds			
Weld Shear	15702	21000	.34
3.6 Bottom Grid Base Plate Weld			
Weld Shear	15941	21000	.32

* Thermal Plus OBE Stress is Limiting

** Allowable Per Appendix XVII - 2215 Eq. (24)

4. b. Continued:

REGION 1 RACKS

SUMMARY OF DESIGN STRESSES AND MINIMUM MARGINS OF SAFETY

Normal & Upset Conditions

		Design Stress (psi)	Allowable Stress (psi)	Margin of Safety
1.0	Grid Assembly - Cont'd			
3.7	Bottom Grid Outer Member			
	Axial and Bending	12050	13890	.15
	Shear	768	9260	11.06
3.8	Base Plate Stiffener to Base Plate Weld			
	Weld Shear	13500	21000	.56

REGION 2 RACKS

SUMMARY OF DESIGN STRESSES AND MINIMUM MARGINS OF SAFETY

Normal & Upset Conditions

		Design Stress (psi)	Allowable Stress (psi)	Margin of Safety
1.0	Support Pad Assembly			
1.1	Support Pad			
	Shear	3504	23150*	5.61
	Axial and Bending	10288	23150*	1.25
	Bearing	7631	23150*	2.03
1.2	Support Pad Screw			
	Shear	6974	9260	.33
1.3	Support Plate			
	Shear	4403	9260	1.10
	Weld Shear	34591	46300*	.34
2.0	Cell Assembly			
2.1	Cell			
	Axial and Bending	.899	1.0†	.11
2.2	Cell to Base Plate Weld			
	Weld Shear	15482	21000	.36
2.3	Cell to Cell Weld			
	Weld Shear	18389	23150*	.26
2.4	Cell Seam Weld			
	Weld Shear	1751†	2194††	.25
2.5	Cell to Wrapper Weld			
	Weld Shear	10299	18520**	.80

* Thermal Plus OBE Stress is Limiting
** SSE Stress is Limiting
† Allowable per Appendix XVII-2215 Eq (24)
†† Design Load and Allowable Load in Lbs is Shown

5. With regard to the simplified 2-D nonlinear model, please respond to the following:

   a. Describe how the seismic loads were applied onto the model.

      RESPONSE: The seismic loads were applied onto the model as simultaneous vertical and horizontal acceleration time histories.

      The analytical model of the fuel assembly used in this model was verified by comparison to fuel assembly test data. The first test was a natural frequencies test to verify model's beam properties and the rotary spring stiffnesses. The second test consisted of the fuel assembly in air impacting on a rigid surface to determine the fuel assembly grid impact stiffness and impact damping values.

   b. Discuss how this model could be used to simulate the 3-D nonlinear structural behavior exhibited by the fuel rack.

      RESPONSE: The nonlinear analysis is performed on a 2-D finite element model using a time history input of a horizontal shock and a vertical shock. The linear model used in the analysis is a 3-D model which is run for two horizontal directions. The loads for each horizontal direction are adjusted by load factors from the nonlinear analysis, and thus include the effects of both a horizontal and a vertical event. The results of the two direction loads are then combined by the SRSS to account for the three seismic events.

   c. Discuss how the time step of integrations was established in the analysis concerning the solution stability and convergence.

      RESPONSE: A time step study is performed for a range of time steps. From the results of this study, it is possible to determine the time step which gives a converged solution. Refinement of the time step beyond this value will not significantly affect the results.

   d. Provide description of the friction element used in the model. Elaborate on whether the friction element is capable of reversing the direction of its restraining force when sliding changes direction.

      RESPONSE: The three-dimensional dynamic friction element is composed of a gap in series with a parallel combination of impact spring and impact damper with a frictional spring orthogonal to the gap. This element is designed to represent two surfaces which may slide relative to each other, and may separate or contact each other. This element is used to model the support pads and the fuel base. This friction element is capable of reversing the direction of its restraining force when sliding changes direction.

   e. Describe the procedure used to calculate the hydrodynamic coupling masses.

      RESPONSE: Hydrodynamic Effects Between Racks - The close proximity of adjacent racks, as well as the size of the racks relative to the gap between racks, is such that extremely large hydrodynamic masses are produced if the racks attempt to respond out of phase.

5. e. CONTINUED

This large hydrodynamic coupling force limits the deflection (and stresses) of racks that attempt to respond out of phase. Thus the limiting condition is the racks responding in phase. (Note that even if the racks could respond out of phase at their maximum displacement the clearances shown in question 4 are large enough to preclude rack to rack impacting.) The seismic analysis for the Turkey Point racks treats the racks as if they are hydrodynamically coupled (move in phase). The hydrodynamic coupling mass between the rack modules and the pool wall was calculated by evaluating the effects of the gap between the modules and the pool wall using the method outlined in the paper by R. J. Fritz. ("The Effect of Liquids on the Dynamic Motions of Immersed Solids" Journal of Engineering for Industry, February 1972.)

6. With regard to the detailed 3-D linear model, please respond to the following:

a. Explain in detail how the load correction factors are derived.

RESPONSE: The nonlinear model accurately represents the non-linearities of the fuel to cell interaction and the interface between the rack base and pool floor (potential lift off and sliding). As a result, the nonlinear model accurately predicts the loads at the rack to environment interface (rack base loads).

The linear model accurately represents the load and stress distribution in the cells and rack structure within the rack module.

The load correction factors based upon the loads at the interface between the rack base and pool floor are used to adjust the overall stresses within the linear model in order to account for the nonlinear effects incorporated in the nonlinear analysis. The load correction factors are determined based on the ratio of the rack base to pool floor interface loads obtained in the nonlinear analysis to the loads obtained in the linear analysis.

b. Discuss how the seismic loads were applied onto the model.

RESPONSE: See response to 5.b of this report.

7. Please provide detailed results on the overturning analysis.

RESPONSE: The nonlinear analysis showed that these racks did not lift off the embeds during the seismic event, thus insuring the stability of the racks.

8. In Section 4.6.4(1), you discuss the fuel drop accident. However, the discussion did not mention the consequences resulting from the fuel assembly drop accident on the pool liner and on the fuel rack structural integrity. Please comment.

RESPONSE: In the analysis it is shown that the energy of the falling fuel assembly is satisfactorily absorbed by the crushing of the fuel rack base plate and the deformation of the lower portion of the fuel assembly (lower fitting and lower portion of the guide tubes and instrument tube). The load transmitted to the pool liner is such that the stress developed in the liner does not result in perforation. It should be noted that the analysis performed is conservative in that the fuel assembly is assumed to be under free fall (water resistance within the cell, is neglected), and it is assumed that no energy is dissipated by the breaking of welds which hold the base plate to the rest of the rack.

8. CONTINUED:

Rack deformation due to the drop accident does not compromise the subcriticality requirements as a Keff less than 0.95 is maintained.

9. Please provide more detailed information about the finite element model of spent fuel pool structure including the stainless steel liner plate elements and how it is connected to the pool walls and foundation mat.

RESPONSE: The spent fuel pool is modeled using three-dimensional solid elements and the ANSYS computer code (Reference 1). Figures 1 through 7 (submitted in response to Question 10) define the model geometry. Due to symmetry along the long direction of the pool (north-south), only half the pool is modeled. A minor geometrical dissymmetry occurs at the west end of the canal area where the spent fuel enters from the reactor building (see Updated FSAR Appendix 14E, Figure 3.1-3). This minor dissymmetry has negligible effect on the structural behavior of the model considered. Conservatively, the stainless steel liner is not considered in the model. The model is supported vertically on a bed of compression spring elements representing the soil stiffness under the structure. (Section 4.5.1 of the Spent Fuel Pool Rerack Safety Analysis Report incorrectly states that the foundation's support is represented by solid elements.)

For symmetric loading of dead load, hydrostatic pressure, vertical earthquake, and spent fuel rack loading, the nodes on the plane of symmetry are restrained in the directions perpendicular to this plane. For the earthquake applied in the north-south direction, similar boundary conditions are employed except that the nodes under the base mat along the perimeter walls are restrained horizontally in the north-south direction. For the nonsymmetric loading associated with the east-west earthquake, the restraints on the nodes in the plane of symmetry are released and the reactions from the symmetric load case are applied with appropriate east-west direction earthquake loads at these released nodes. For load cases which include east-west seismic loading, the nodes under the base mat around the perimeter walls are restrained horizontally in the east-west direction. Inertia loads due to the earthquake directly attributed to the concrete are input as distributed body forces. All symmetric loads are applied simultaneously with the earthquake loads for each of the four directions (north, south, east, and west).

Thermal loads are applied as a separate load case with boundary conditions similar to those for the symmetric loads without horizontal earthquake. No additional loads are imposed on the structure in the thermal load case except for horizontal forces between the mat and the soil springs which represent the effect of friction between the soil and the base mat caused by thermal growth.

These individual load effects are combined as discussed in response to Question 10.

REFERENCE: 1. G. J. DeSalvo and J. A. Swanson, "ANSYS Engineering Analysis System," Swanson Analysis Systems, Inc., July, 1979.

10. Please provide a summary of the stress analysis of the spent fuel pool structure (walls, foundation mat, and liner plates), also the bearing stress of the soil and bed rock supporting the pool.

RESPONSE: The stress analysis was performed in accordance with the criteria included in the Turkey Point Updated FSAR, Appendix 5A, Section II (Design Bases). In summary, this criteria includes the following for Category I structures outside the containment;

$$Y = 1/\phi\,(1.25D + 1.25E)$$

$$Y = 1/\phi\,(1.25D + 1.0R)$$

$$Y = 1/\phi\,(1.25D + 1.25H + 1.25E)$$

$$Y = 1/\phi\,(1.0D + 1.0E^{1})$$

where Y = required yield strength of the structures.

D = dead load of structure and equipment plus any other permanent loads contributing stress, such as soil or hydrostatic loads. In addition, a portion of "live load" is added when such load is expected to be present when the unit is operating. An allowance is also made for future permanent loads.

R = force or pressure on structure due to rupture of any one pipe.

H = force on structure due to restrained thermal expansion of pipes under operating conditions.

E = design earthquake load

E^{1} = maximum earthquake load

W = wind load (to replace E in the above load equations whenever it produces higher stresses).

Per the FSAR, design is in accordance with ACI 318-63. These criteria were used to evaluate the structure for effects from the replacement fuel racks. (Note that the Spent Fuel Storage Facility Modification Safety Analysis Report incorrectly states that SRP Section 3.8.4 and the NRC OT Position Paper were also employed in this evaluation.)

The analysis consisted of obtaining the state of stress in the pool using the analytical model described in the response to Question 9. Dead weight, hydrostatic pressure, and spent fuel rack loadings on the pool were considered separately and in combination with seismic, thermal, and wind loads to satisfy the following load combinations:

1. 1.25 (D + P + L) with and without T
2. 1.25 (D + P + L) with and without W
3. 1.25 (D + P + L + E) with and without T
4. 1.0 (D + P + L + E^{1}) with and without T

10. CONTINUED:

where,

D = weight of the structure
P = hydrostatic pressure of pool water
L = weight of loaded fuel racks in pool
E = design earthquake load, 0.05 g horizontally
2/3 (0.05 g) vertically
E^{I} = maximum earthquake load, 0.15 horizontally
2/3 (0.15 g) vertically
T = thermal loads
W = wind loads

By using enveloping considerations, these load combinations were reduced to the following controlling load combinations:

1.25 (D + P + L) with and without T
1.25 (D + P + L) + E^{I} with and without T

Seismic input loads for the analysis of the pool structure were obtained using the results of the seismic analysis discussed in FSAR Appendix 14E, Section 3.2. Seismic loads for the new racks were taken into account in the pool structural evaluation. Because analysis has shown that these racks do not uplift during the seismic event, no added amplification factor for impact was considered.

Analysis showed that the seismic loading created a more severe effect than the combined effect of tornado wind and depressurization.

The thermal effect was obtained by imposing a uniform thermal gradient across the solid elements. In accordance with FSAR Section 5.2.3, the temperature of the inside face of the pool was taken as 180°F while that of the exposed outside face of the walls was taken as 30°F. The temperature of the bottom face of the slab was taken as 50°F. This represents the effect after thermal equilibrium is reached. Based on the methodology suggested in Reference 1, Appendix A, this represents a worst case design condition.

Representative critical elements of the finite element model in the base mat and all walls were identified based both on high stress results and locations which result in severe loading. These elements are shown in Figures 3 through 7 and were further evaluated in the manner described below:

1. Resulting stresses in elements caused by mechanical loads (all identified loads in the load case except thermal loads) were evaluated by computing the capacities of the individual sections and comparing the capacities to the actual normal forces and moments.

2. For the combination of mechanical and thermal loads, the sections were analyzed in accordance with the methodology discussed in Reference 2, Section 2.5.6.3.3 and Appendix A.

10. CONTINUED:

A summary of the controlling stresses is provided in Table A for the locations identified in Figures 3 through 7. These stresses represent maximum stresses for load transfer. Controlling stresses occur in reinforcing steel, except for one instance where concrete shear governs.

The average bearing stress under the mat is 5 ksf, with a localized maximum of 9 ksf. This is below the design allowable pressure of 10 ksf for the compacted limerock fill. The average bearing stress on the bedrock, approximately 20 feet below the mat foundation, is also 5 ksf, with a conservatively computed localized maximum of 7.4 ksf. This is below the design allowable pressure of 7.5 ksf. This value accounts for the weight of the limestone backfill under the mat.

The liner plate was not considered to provide structural resistance in the analysis of the spent fuel pool. However, a separate analysis was conducted to determine the effects of thermal, hydrostatic and hydrodynamic loads on the functionality of the liner system. This analysis reviewed the buckling potential of the liner plate, as well as stresses in welds and embeds associated with it. The analysis shows that there will be no loss of function.

The reported analysis, as indicated above, was conducted on the assumption of a maximum water temperature of 180°F, based on the updated FSAR criteria. Recent evaluations using more conservative criteria indicate that the maximum water temperature may reach 183°F. By comparing the results of the analysis performed for 180°F water temperature with that performed for 212°F water temperature (see response to NRC Question No. 8 submitted to Florida Power and Light via NRC letter of September 6, 1984), an upper bound interpolation indicates that the maximum stresses reported would not be increased by more than 0.5 ksi if the water temperature were assumed to be 183°F. This increase results in stress levels which remain within the specified allowables.

References:
1. Commentary to ACI 349R-80
2. ACI Committee 349 Report Criteria for Reinforced Concrete Nuclear Power Containment Structure, ACI Journal 1972.

TABLE A

LOAD COMBINATION

	MECHANICAL LOADS								MECHANICAL & THERMAL	
	1.25 (D + P + L)				1.25 (D + P + L) + E				1.25 (D + P + L) + E + T	
			(1)				(1)		(2)	(3)
Location	N (K/ft)	M K-ft/ft	M_m K-ft/ft	Mm/M	N (K/ft)	M K-ft/ft	M_m K-ft/ft	Mm/M	Rebar Stress	ØFY / Rebar Stress
Base Mat	18.1	7.8	23	2.95	13.2	16.7	27	1.6	fs = 12.8 ksi (5)	2.81
East Wall (Canal)	9.6	-22 (fv = 82 psi)	-52	2.36 1.80(4)	25.0	-29.3 (fv = 142 psi)	-43	1.47 1.04 (4)	fv = 142 psi (6)	1.04 (4)
East Wall (Pool)	33.2	122	568	4.66	64.6	163	490	3.0	fs = 35.1 ksi f's = -9.6 ksi	1.03
North Wall	19.8	-96.6	-123	1.27	13.1	-140	-151	1.08	fs = 27.1 ksi f's = -2.65 ksi	1.33
South Wall	18.9	-38.5	-192	4.99	23.0	-76.1	-182	2.39	fs = 35.3 ksi(7) f's = 1.4 ksi	1.02
Middle Wall	28.5	22.1	209	9.46	2.6	32.5	218	6.7	fs = 9.6 ksi f's = 9.0 ksi	3.75

N = Applied normal force on section
M = Applied moment on section
M_m = Maximum elastic moment
(negative sign indicates compressive stress)

fs = Stress in tension steel
f's = Stress in compression steel
fv = Concrete shear stress

NOTES:

(1) Maximum elastic moment for a section with normal force N imposed on it.

(2) Based on a cracked analysis per the methodology discussed in Reference 2, reinforcing steel stress is obtained directly.

TABLE A (continued)

(3) Due to the self relieving nature of thermal loads on reinforced concrete, the ratio of maximum moment capacity to actual moment cannot be uniquely determined. As an alternative, the ratio of ϕFy to computed reinforcing steel stress is provided. Since structural integrity is maintained beyond the allowable stress for thermal loading, the actual safety factor is greater than the ratio reported.

(4) Where shear stresses control, the ratio provided is that of allowable shear stress (conservatively taken as 148 psi) divided by f_v.

(5) This stress represents the maximum stress found in the top layer of reinforcing steel in the thinner center section of the base mat. The top steel in this area is important for transfer of the tensile loads imposed by the lateral water pressure from the pool. The bottom steel in the center portion of the base mat of the pool is used primarily for crack control. Since the base mat rests directly on competent fill material, stresses in this bottom (secondary) steel resulting from thermal loads have no adverse effect on the ability of the pool to transfer load. Therefore, the stress in the bottom steel is not included in Table A.

(6) As shown in Figure 6, this section occurs in the 3 foot wide by 18 inch thick section of the east wall between the two canal walls. Because of the short span of this section, and the large ratio of section thickness to span length, the section does not resist loads in the fashion of a shallow beam; shear stresses control the section capacity. Since shear stirrups are provided, the allowable shear stress in the concrete exceeds 148 psi. The reinforcing steel on the outside face of this section is used only for crack control and is not needed to resist mechanical loads. Therefore, the flexural stresses in this reinforcing steel are not included in Table A.

(7) This represents an average stress (total force on the total section) over the top 10 feet of the outside face horizontal reinforcing steel. The result indicates that the section in general remains below the minimum specified yield stress. However, a maximum stress of 38 ksi has been calculated for the reinforcing steel in the top element of the wall. Realizing the self-relieving nature of the thermal stresses and further acknowledging that the section in general remains elastic, pool function and structural integrity are maintained.

QUESTION 10 (Continued)

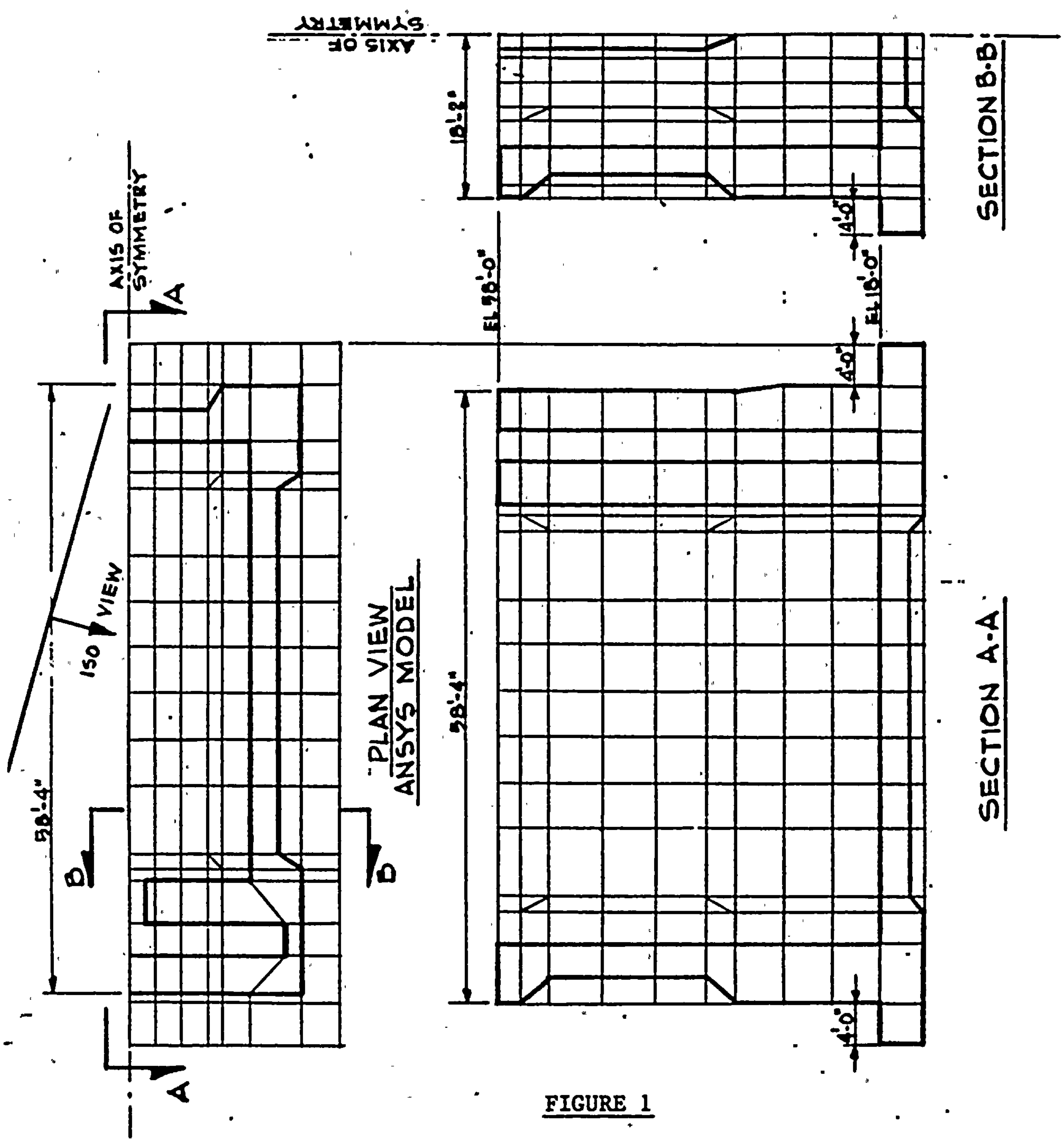

FIGURE 1

QUESTION 10 (Continued)

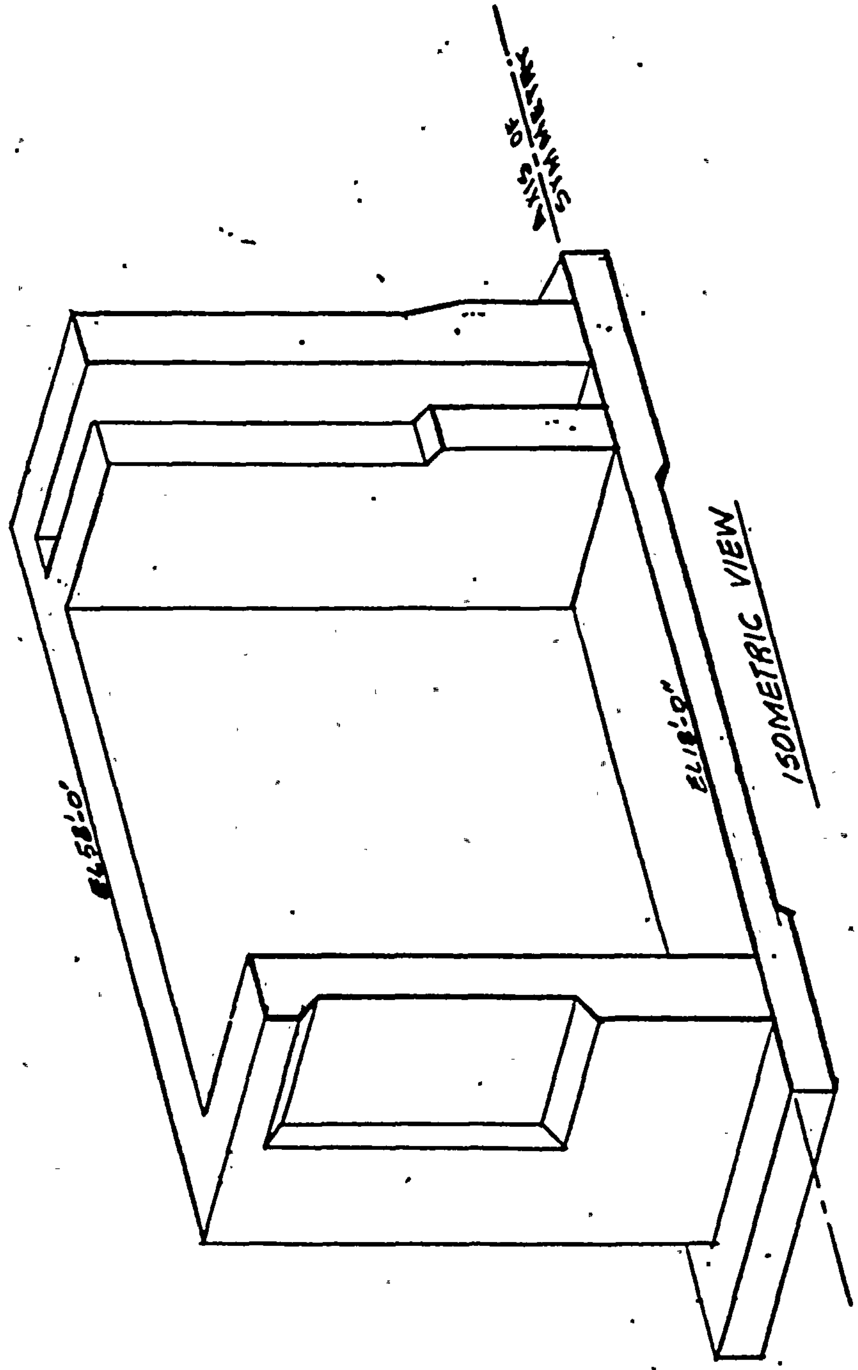

FIGURE 2

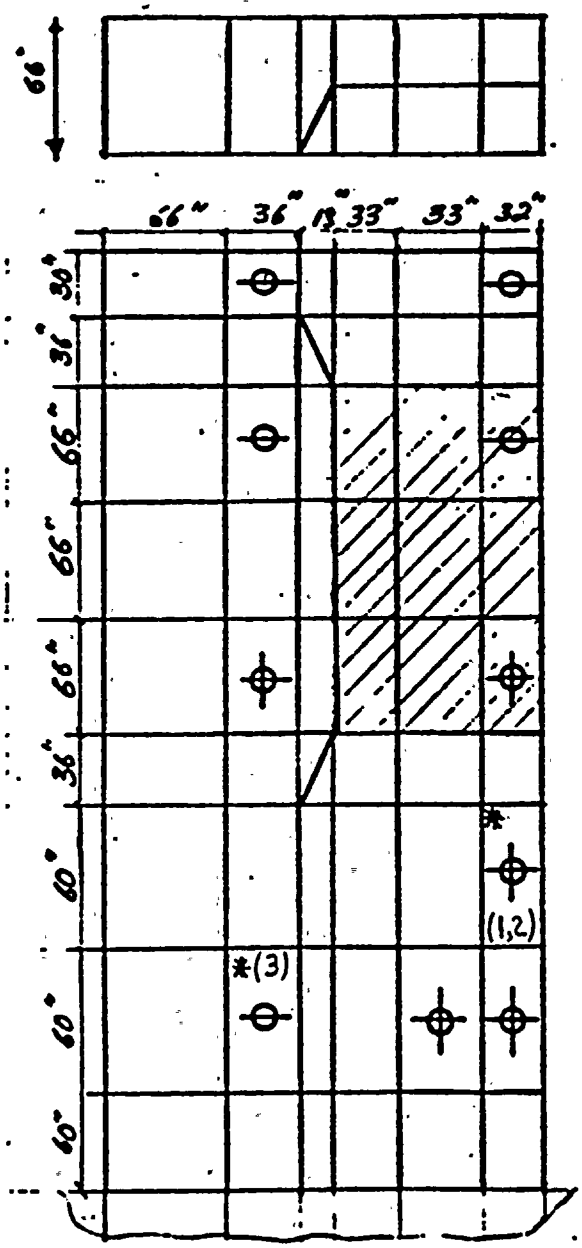

NORTH WALL
(Looking South)

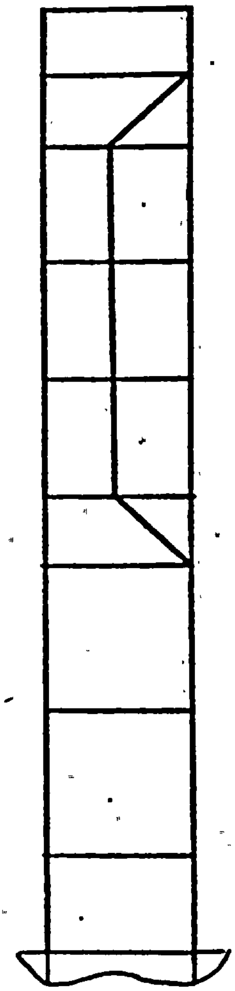

SIDE VIEW
(Looking West)

LEGEND

—⊖—	Stresses evaluated in horizontal direction
⏀	Stresses evaluated in vertical direction
✱	Location of governing stress reported in Table A
( )	Number in parentheses indicates governing load combination number in table A.

FIGURE 3

QUESTION 10 (Continued)

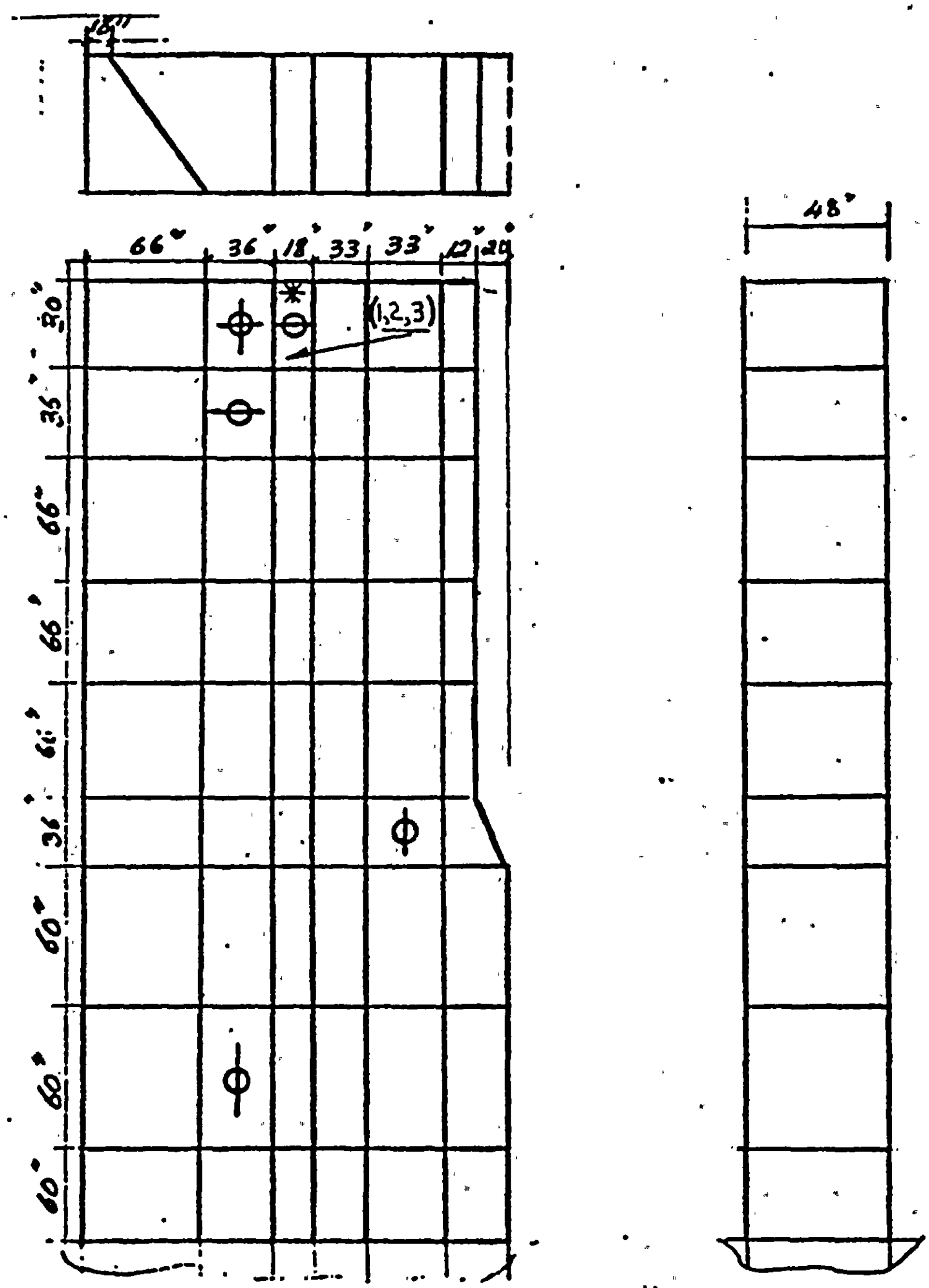

MIDDLE WALL
(Looking south)

(For legend, see Figure 3)

FIGURE 4

QUESTION 10 (Continued)

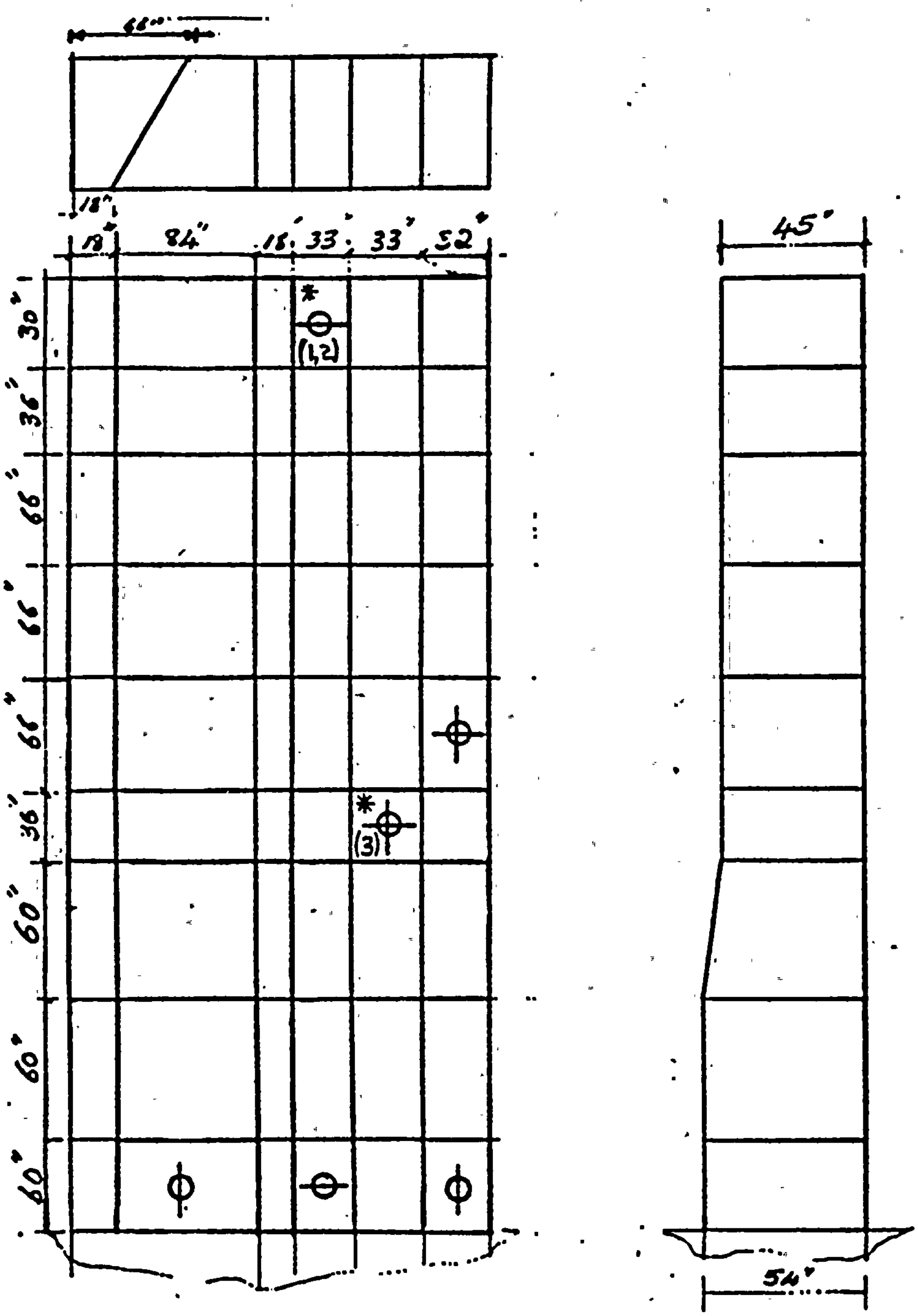

SOUTH WALL
(Looking South)

(For legend, see Figure 3)

FIGURE 5

QUESTION 10 (Continued)

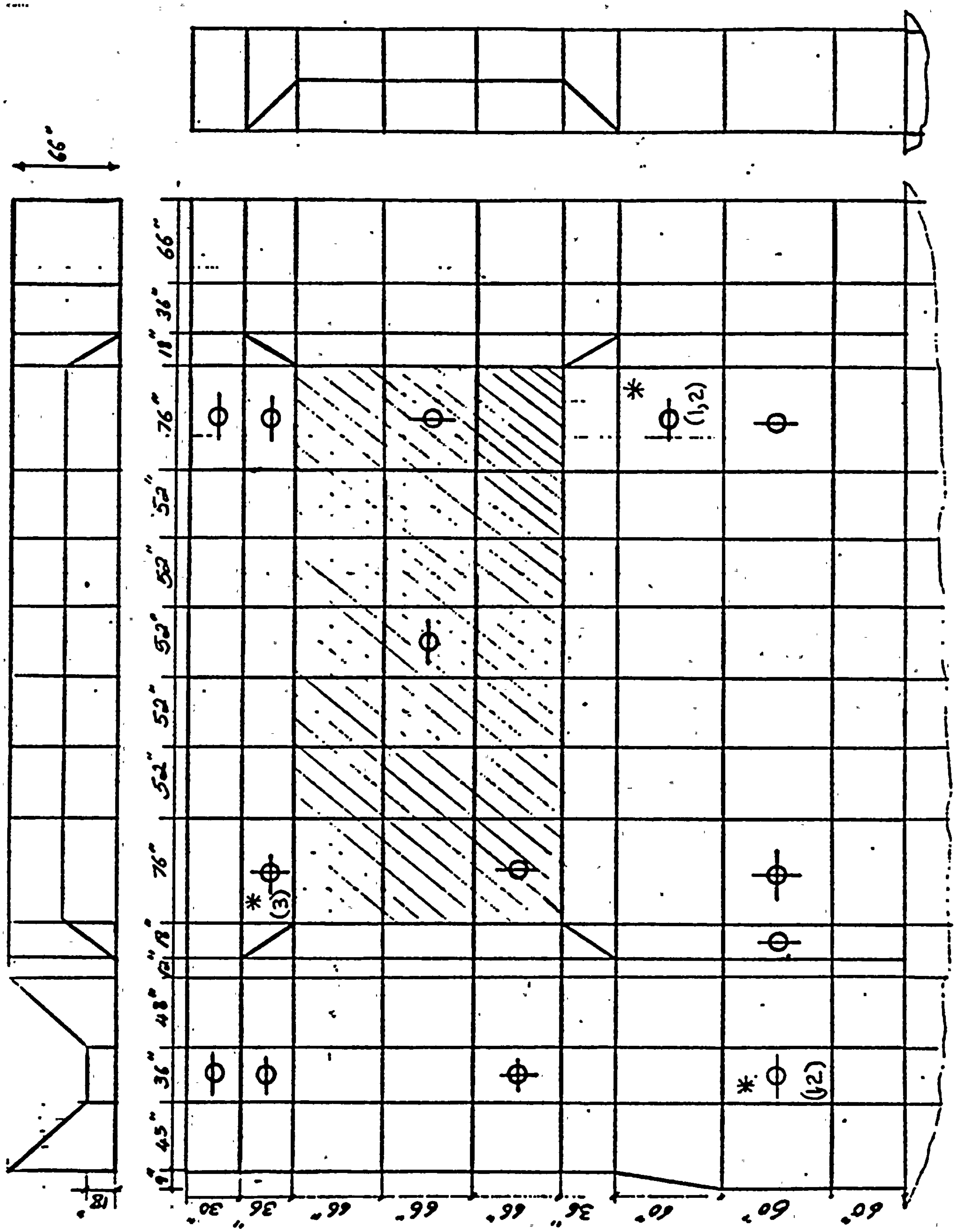

EAST WALL (Looking West)

FIGURE 6

(For legend, see Figure 3)

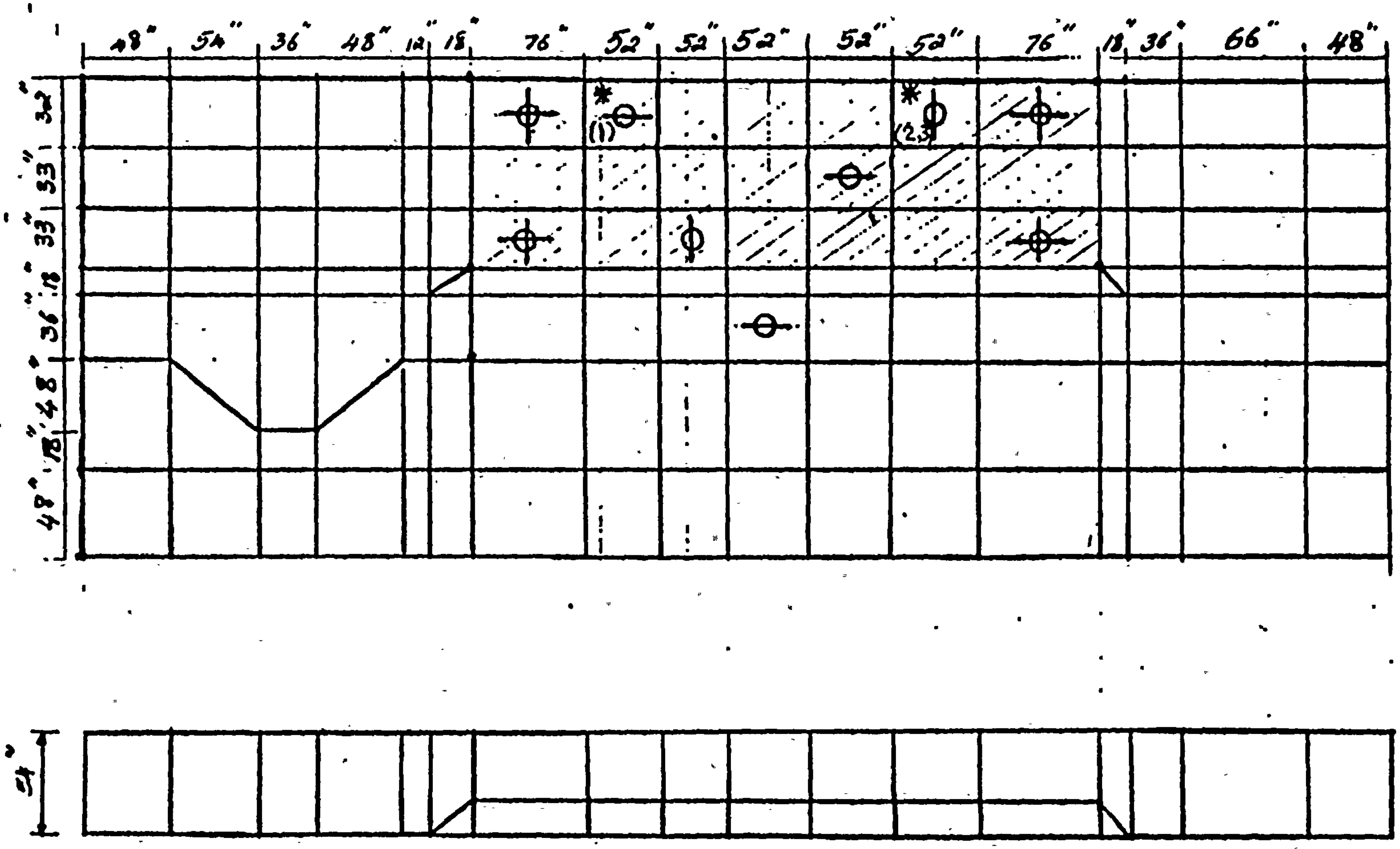

BASE MAT

(For legend, see Figure 3)

FIGURE 7

11. Provide a sample calculation of the ultimate strength design of the critical connection between the pool well and the foundation mat. Have the reinforced concrete and stainless steel liner plate been considered as a composite section in this analysis?

RESPONSE: The ultimate strength design approach as defined by ACI 318 was not used. Conservatively, the acceptable ACI alternative of working stress, utilizing minimum specified yield strength for reinforcing steel, was used for all sections in the pool (including the connection between the wall and the foundation mat) as follows:

- For each section of the structure, section properties (thickness, reinforcing steel area, depth, etc.) are determined and the section capacities for the combination of moment and axial forces are established.

- The capacities are computed by use of the following equilibrium equations for combined moment and axial forces:

$$\Sigma F = 0: \quad (\tfrac{1}{2} f_c bkd) + A_s' f_s' - A_s f_s = P$$

$$\Sigma M_P = 0: \quad (\tfrac{1}{2} f_c bkd)\left(e - \frac{t}{2} + \frac{kd}{3}\right) + A_s' f_s' \left(e - \frac{t}{2} + d'\right) - A_s f_s \left(e - \frac{t}{2} + d\right) = 0$$ Reference 1

where

b = unit width of the section = 12 in

d = depth of the section from the extreme compression fiber to the center of tension steel

d' = distance from the extreme compression fiber to the center of compression steel

k = factor where kd is the distance from the extreme compression fiber to the neutral axis of the effective section

e = eccentricity from neutral axis to the assumed location of axial force to produce moment on the section

t = total thickness of the section

As = area of tension steel

A's= area of compression steel

fc = concrete stress

f's= compression steel stress

fs = tension steel stress

P = axial force on the section (tension or compression)

11. CONTINUED:

This constitutes two equations with two unknowns (P and e). Moment capacity is computed as (P) x (e).

- For each value of k in the equations, there correspond values for P and e (and consequently M).
- The solution for the two equations is coded and the equations are solved for incremental values of k. The resulting combinations of moments and axial forces for each section are tabulated as shown in Table A.
- The actual moment and normal force combinations from the structural analysis of the pool are computed and compared to the capacity of the corresponding section as determined above. The section is considered adequate when the actual moment and normal force combination is equal to or less than the moment and normal force capacity of the section..
- Shear stresses in the section are separately compared to allowable concrete shear stresses per ACI 318.
- Allowable concrete and steel stresses (compression, tension, bending and shear) are not exceeded at the connection between the walls and foundation mat.
- The liner plate has not been considered to act in a composite manner with the concrete, and has therefore been neglected in this analysis.

Reference: 1. K.H. Gerstle, "Basic Structural Design", McGraw-Hill Book Co., 1967.

TABLE A

SECTION MOMENT AND AXIAL FORCE CAPACITY

EAST WALL ELEM. 251 X-DIRECTION

SECTION PROPERTIES ARE H = 66.00	D1 = 64.00	D2 = 2.00
LIMITING STRESSES ARE FS = 36.00	FSP = 36.00	FC = 2.55
STEEL PROPERTIES ARE NR = 9.09	A1 = 3.56	A2 = 3.02

K2	FS KSI	FSC KSI	FC KSI	P K/FT	M K-FT/FT
.100	36.00	-5.50	-.44	94.65	417.45
.105	36.00	-5.93	-.46	91.51	425.39
.110	36.00	-6.37	-.49	88.24	433.60
.115	36.00	-6.81	-.51	84.86	442.09
.120	36.00	-7.26	-.54	81.34	450.86
.125	36.00	-7.71	-.57	77.71	459.91
.130	36.00	-8.17	-.59	73.94	469.25
.135	36.00	-8.64	-.62	70.04	478.88
.140	36.00	-9.10	-.64	66.00	488.80
.145	36.00	-9.58	-.67	61.85	499.01
.150	36.00	-10.06	-.70	57.53	509.53
.155	36.00	-10.54	-.73	53.08	520.34
.160	36.00	-11.04	-.75	48.48	531.45
.165	36.00	-11.53	-.78	43.75	542.87
.170	36.00	-12.04	-.81	38.86	554.60
.175	36.00	-12.55	-.84	33.82	566.64
.180	36.00	-13.06	-.87	28.65	579.00
.185	36.00	-13.58	-.90	23.28	591.67
.190	36.00	-14.11	-.93	17.77	604.67
.195	36.00	-14.69	-.96	12.00	617.99
.200	36.00	-15.19	-.99	6.25	631.64
.205	36.00	-15.78	-1.02	.25	645.62
.210	36.00	-16.29	-1.05	-5.93	659.94
.215	36.00	-16.85	-1.08	-12.29	674.61
.220	36.00	-17.42	-1.12	-18.82	689.61
.225	36.00	-18.00	-1.15	-25.54	704.96
.230	36.00	-18.58	-1.18	-32.45	720.67
.235	36.00	-19.18	-1.22	-39.54	736.73
.240	36.00	-19.78	-1.25	-46.82	753.16
.245	36.00	-20.38	-1.29	-54.31	769.94
.250	36.00	-21.00	-1.32	-61.99	787.10
.255	36.00	-21.62	-1.36	-69.88	804.64
.260	36.00	-22.26	-1.39	-77.98	822.55
.265	36.00	-22.90	-1.43	-86.29	840.85
.270	36.00	-23.55	-1.46	-94.83	859.54
.275	36.00	-24.21	-1.50	-103.58	878.62
.280	36.00	-24.87	-1.54	-112.56	898.11
.285	36.00	-25.55	-1.58	-121.77	918.00
.290	36.00	-26.24	-1.62	-131.22	938.30
.295	36.00	-26.94	-1.66	-140.91	959.02
.300	36.00	-27.64	-1.70	-150.85	980.17
.305	36.00	-28.36	-1.74	-161.04	1001.74
.310	36.00	-29.09	-1.78	-171.49	1023.75
.315	36.00	-29.82	-1.82	-182.20	1046.20
.320	36.00	-30.57	-1.86	-193.19	1069.11
.325	36.00	-31.33	-1.91	-204.46	1092.47
.330	36.00	-32.10	-1.95	-215.98	1116.29
.335	36.00	-32.89	-2.00	-227.81	1140.59
.340	36.00	-33.69	-2.04	-239.93	1165.36
.345	36.00	-34.49	-2.09	-252.35	1190.63
.350	36.00	-35.31	-2.13	-265.08	1216.38

ACTUAL ENVELOPING LOADS

P = 64.6 k/ft
M = 163 k-ft/ft

P = 33.2 k/ft
M = 122 k-ft/ft

12. Please discuss the design of the weld connections between the stainless steel liner plates.

RESPONSE: The 1976 liner repair/replacement and acceptance criteria are discussed in Updated FSAR Section 14E. The liner plate is not a structural element. The loading from the stored fuel is transferred to the concrete mat through the embedded plates. The liner plate was not designed to act with the concrete as a composite section. Monitoring trenches are provided behind the liner for detecting and collecting any leakage. Any leakage is directed to the waste disposal drainage system, thus preventing uncontrolled leakage of fuel pool water.

In support of the leak prevention function, the liner plates are welded to each other or to embedded plates using seam welds which were sized for hydrostatic and thermal loads. Vertical seams in the wall liner plates are square butt or bevel butt welds with embedded 1/4" x 2" continuous bars serving as backing bars (Figures 1 and 2). Horizontal seams in the wall liner plates are fillet welds between the plate edges and the embedded 1/4" x 21" continuous bars (Figure 3). Seams in the floor liner plate are fillet welds between plate edges and embedded plates or bars. The surfaces of the seams are maintained flush with the floor by use of 1/4" square filler bars and bevel filler welds (Figure 4).

QUESTION 12 (Continued)

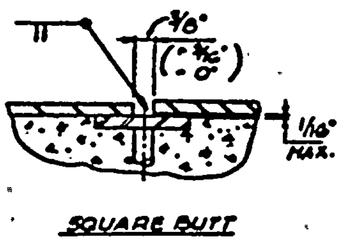

FIGURE 1

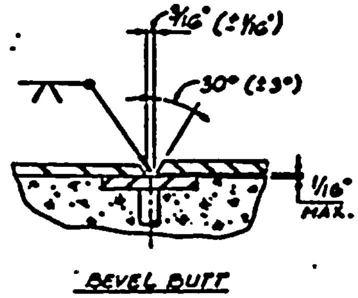

FIGURE 2

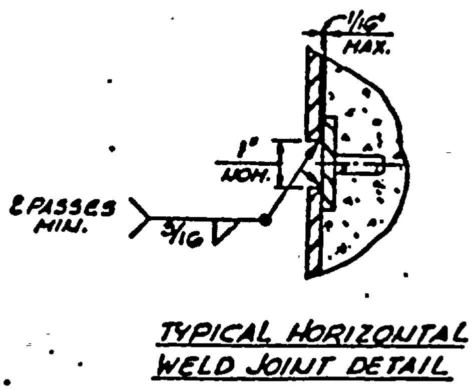

FIGURE 3

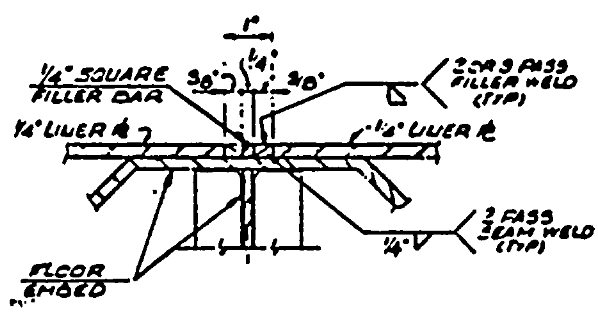

FIGURE 4